IOP Conf. Series: Materials Science and Engineering **529** (2019) 012018 doi:10.1088/1757-899X/529/1/012018

Cellular-to-Dendritic and Dendritic-to-Cellular Morphological Transitions in a Ternary Al-Mg-Si Alloy

C. Brito[1], H. Nguyen-Thi[2], N. Mangelinck-Noël[2*], N. Cheung[3], J.E. Spinelli[4], A Garcia[3]

[1] Campus of São João da Boa Vista, São Paulo State University, UNESP, 13876-750 São João da Boa Vista/SP Brazil.
[2] Aix-Marseille Université, CNRS, IM2NP UMR CNRS 7334, Campus Saint Jérôme, case 142, 13397 Marseille Cedex 20, France.
[3]Department of Manufacturing and Materials Engineering, University of Campinas, UNICAMP, 13083-970 Campinas/SP, Brazil.
[4]Department of Materials Engineering, Federal University of São Carlos – UFSCar, 13565-905 São Carlos/SP, Brazil.
*E-mail: nathalie.mangelinck@im2np.fr

Abstract. The study is focused on the influence of solidification thermal parameters upon the evolution of the microstructure (either cells or dendrites) of an Al-3wt%Mg-1wt%Si ternary alloy. It is well known that the application properties of metallic alloys will greatly depend on the final morphology of the microstructure. As a consequence, various studies have been carried out in order to determine the ranges of cooling rates associated with dendritic-cellular transitions in multicomponent alloys. In the present research work, directional solidification experiments were conducted using either a Bridgman (steady-state) device or another device that allows the solidification under transient conditions (unsteady-state). Thus, a broad range of cooling rates ($\dot{T}$), varying from 0.003K/s to 40K/s could be achieved. This led to the identification of a complete series of cellular/dendritic/cellular transitions. For low cooling rate experiments, low cooling rate cells to dendrites transition happens. Moreover, at a high cooling rate, a novel transition from dendrites to high cooling rate cells could be observed for the Al-3wt%Mg-1wt%Si alloy. Additionally, cell spacing λ_C and primary dendritic spacing λ_1 are related to the cooling rate by power function growth laws characterized by the same exponent (-0.55) for both steady-state and unsteady-state solidification conditions.

1. Introduction

The microstructural morphology in metallic alloys is of prime importance. Properties such as mechanical strength, corrosion resistance and wear resistance were proved to be affected by the morphology and scale of the α-Al matrix. Then, due to the direct relationship observed between the solidification microstructure and the final properties, several experimental studies and models were devoted to the conditions in which the morphology of the solid-liquid (S/L) interface changes. The solid-liquid interface instability depends on the growth rate, the thermal gradient and the distribution of solute ahead of the S/L interface leading to the constitutional undercooling [1-10].

The constitutional undercooling criterion is largely used to predict whether a S/L planar interface is stable or not, despite showing some important limitations. Firstly, the constitutional undercooling is based on thermodynamic equilibrium considerations, whereas the evolution of the S/L interface during solidification is a non-equilibrium process. Secondly, the local curvature of the interface is not taken

into account although it can impact the free energy of the system. Thirdly, the evolutionary trend of the interface morphology is not described. This criterion is not valid for rapid solidification or processes involving non-equilibrium solidification.

Hunt and Lu [1] developed a numerical model for the growth of cells and dendrites that predicts the transition between these two types of microstructures. This transition was considered diffuse. It ends when the preferred direction of growth is reached and the secondary dendritic arms are already defined.

Although the specialized literature shows investigations about the transitions regarding the sequence planar - cellular - dendritic - cellular - planar, few studies were devoted to the reverse dendritic to cellular microstructural transition in multicomponent metallic alloys. Most of the studies dealt with the cellular to dendritic transition that occurs combining dilute alloys, low growth rate and high temperature gradients. The cellular to dendritic transition with cells known as high-speed cells was only supposed to occur at very high growth rates [2]. However, no consensus on which thermal and compositional parameters are the determinant factors leading to this type of transition has been established to date.

In the present investigation, an Al-3wt%Mg-1wt%Si alloy is directionally solidified (DS) under transient and stationary solidification conditions with a wide range of cooling rates. It is shown that the investigated alloy transitioned from fully cellular to dendritic and from dendritic to cellular for high cooling rates. The microstructural transitions are characterized, and the evolution laws for cellular and the dendritic length scales with the solidification cooling rate are also established.

2. Experimental procedure

In order to obtain a broad range of cooling rates, two solidification systems were used to perform the experiments. A water-cooled directional solidification (DS) setup permitted unsteady-state conditions and high cooling rates to be achieved, whereas a Bridgman type device guaranteed solidification under constant temperature gradient and cooling rate. During the unsteady-state solidification, the alloy was melted *in situ* by radial electrical wiring positioned around a cylindrical stainless steel split mold with inner diameter of 60 mm; height of 150 mm and wall thickness of 5mm. More details about this system can be found elsewhere [8, 11]. The Bridgman setup is built to operate with a cold and a hot part separated by an adiabatic zone. The hot part is constituted by two heating elements wounded around a 15 mm diameter cylindrical alumina piece. In this set-up, the controlled displacement of the crucible inside the furnace is allowed. During the Bridgman furnace experiments, the temperature gradient was fixed at a value of 11K/cm while the solidification rates (v) were varied in the range from 0.3 μm/s to 70 μm/s [11].

The solidification thermal parameters, growth rate (V_L) and cooling rate ($\dot{T}$), during unsteady-state growth were determined from seven type K thermocouples (with 0.2 mm diameter wire) positioned along the length of the DS casting at the positions 3, 6, 12, 20, 30, 50 and 70mm from the metal/mold interface. These sensors were connected by coaxial cables to a data logger interfaced with a computer, capable of automatically record temperature data at a frequency of 5 Hz.

Optical microscopy analyses were performed using an Olympus inverted metallurgical microscope (model 41GX). The cellular (λ_C), primary dendritic arm (λ_1) and secondary dendritic arm (λ_2) spacings were measured from the optical images of transverse and longitudinal section metallographies. The triangle method [12] was used in order to determine λ_C and λ_1 measurements. The intercept method was adopted for measuring λ_2. At least 50 measurements were performed for each sample related to a single cooling rate in both steady and unsteady state regimes.

3. Results and discussion

Figure 1 shows the variations of cellular and primary dendritic spacings with the cooling rate. The range of experimental cooling rates associated with the unsteady-state solidified samples was

$0.2<\dot{T}<45$ K/s. Cooling rates higher than 2 K/s were characterized by the growth of α-Al cells and cooling rates lower than 0.8 K/s are related to the prevalence of α-Al dendrites. The intermediate microstructures, constituted of both cells and dendrites, remained associated with $0.8<\dot{T}<2.0$ K/s.

Additionally, the experiments carried out following steady state conditions have allowed to monitor the influence of the solidification thermal parameters (here synthesized by the cooling rate for easier comparison with the unsteady state experiments) on the final microstructure. From these experiments, the cellular-to-dendritic transition for low cooling rates could be studied. Moreover, a complete description of the cellular→dendritic→cellular transitions for the ternary Al-3wt%Mg-1wt%Si alloy could be deduced. The range of experimental cooling rates during the steady state experiments was $0.003<\dot{T}<0.17$ K/s. For cooling rates between 0.03K/s and 0.17 K/s only typical α-Al dendritic morphologies could be observed. A gradual cellular-to-dendritic transition started to occur for cooling rates lower than 0.03 K/s and ended at about 0.005 K/s. For $\dot{T}<0.005$K/s, no evidence of dendrites could be observed. The range where the aforementioned morphologies prevailed can be seen in Figure 1. The present experimental approach appears to be very practical with a view to determining microstructural morphological transitions in other Al-based multicomponent alloys of interest.

Contrary to the expectations from the literature for metallic systems [13,14], the Al-3wt%Mg-1wt%Si alloy shows high-velocity cells occurring even for moderate $\dot{T}$ values. The length-scale of the cells was observed to be relatively coarse, that is, λ_C varied from 10 μm to 40 μm. Typical dendritic morphologies were observed with λ_1 varying in the range 115 - 270 μm. The length scale of the microstructure is reduced to about 1/3 when the dendritic morphology changes into high-velocity cells.

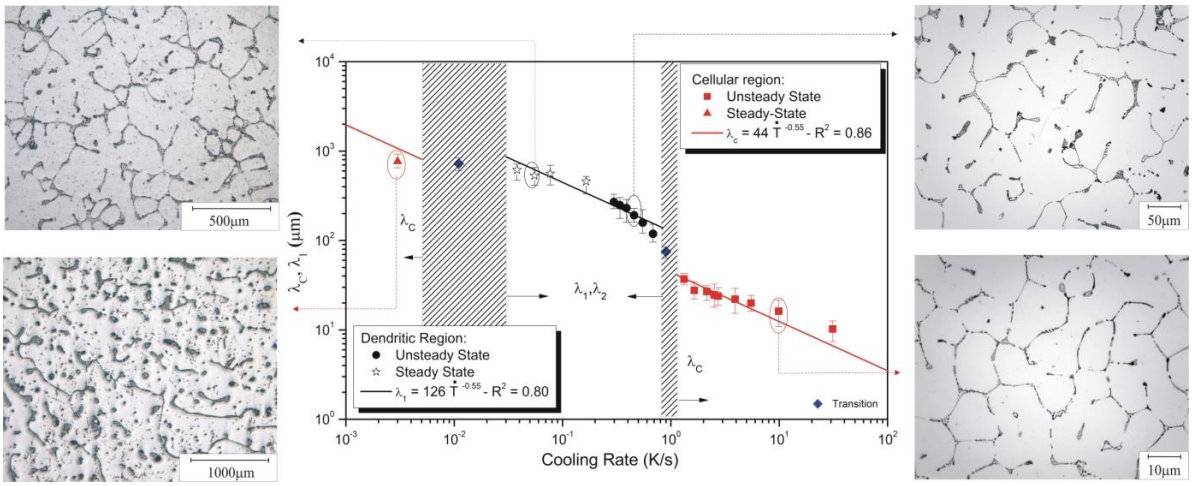

Figure 1 - Variations of cellular and primary dendrite arm spacings with cooling rate and typical transverse microstructures of each α-Al morphological region of directionally solidified Al-3wt%Mg-1wt%Si alloy samples.

The present results allowed comparisons of the experimental scaling laws relating cellular and primary dendrite arm spacing to the cooling rate. The λ_C and λ_1 were related to $\dot{T}$ by power function growth laws characterized by a same exponent of -0.55, that is, $\boldsymbol{\lambda_1 = 44\dot{T}^{-0.55}}$ and $\boldsymbol{\lambda_1 = 126\dot{T}^{-0.55}}$ for cellular and dendritic regions, respectively. Such experimental scaling laws confirm the application of the exponent −0.55 in order to correlate the λ_C and λ_1 evolution with the cooling rate. This exponent has been largely applied for the dendritic growth of a number of binary and ternary metallic alloys [9, 11, 14, 15, 16, 17].

Figure 2 shows the evolution of the secondary dendrite arm spacings against the cooling rate. The experimental scatter is represented by average spacing values with their standard deviations for both samples solidified under steady state and unsteady state regimes. λ_2 decreases with the increase in

cooling rate according to the experimental growth law $\boldsymbol{\lambda_2 = 22\dot{T}^{-0.55}}$, obtained from a fit on the experimental scatters. In a recent study [15], the secondary dendritic growth of a binary Al-3wt.%Mg alloy was shown to be represented by a -1/3 exponent power function growth law. The addition of 1wt%Si seems to change the intensity of lateral solute segregation inside the region corresponding to the secondary arm regions. The addition of Si appears to make λ_2 more sensitive to variations in the solidification cooling rate. Recent research works [14, 16] stated that the effects of lateral solute segregation on the wavelengths of instabilities along the sides of primary dendritic stems for multicomponent alloys are still not well understood. The same exponent, -0.55, was also used to correlate the experimental growth of the secondary dendrite arm spacing against the cooling rate for ternary Al-Cu-Ni alloys [9].

Figure 3 shows a schematic representation of the complete cycle of morphological transitions obtained in the present investigation. An unusual form of transition reported in the literature as the reverse dendritic to cellular shift for metallic systems was observed. For binary systems, the well-known theories from the literature have shown that the cellular-to-dendritic transition is typical of dilute alloys and for lower cooling rates (4, 18). The morphology known as high-speed cells was only supposed to occur at very high growth rates [2, 5]. Further investigations regarding to alloy cooling rate and a variety of solute contents appear to be decisive for the understanding of the occurrence of the reverse transition in multicomponent alloys.

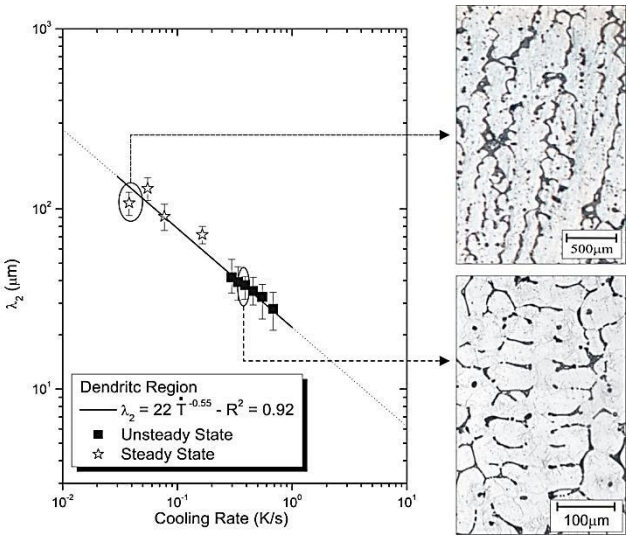

Figure 2 –Variations of secondary dendritic spacing *vs.* cooling rate and typical longitudinal microstructures of each morphological region of the directionally solidified Al-3wt%Mg-1wt%Si alloy samples.

The solid/liquid interface transition (S/L) for the growth of cells and dendrites is explained in terms of the constitutional undercooling criterion for the growth of binary alloys. In this criterion the increase in the alloy solute content (C_0), increase in growth rate (v) and decrease in thermal gradient (G) can induce instabilities at the solid/liquid (S/L) interface [1, 4]. However, there are few available criteria in the literature dealing with multicomponent alloys.

According to the constitutional undercooling criterion, increase in C_0 destabilizes the S/L interface forming instabilities that give origin to the dendritic growth. For multicomponent alloys, the increase in C_0 (or, ΣC_0, sum of all solutes) seems to affect differently. In the case of the examined non-dilute alloy, the sum of the solute chemistries is equal to 4wt.%, which would lead to the growth of a totally dendritic morphology since it does not characterize a dilute alloy. This is not so considering the present experimental results. Cells grew for either $\dot{T}<0.005$ K/s or $\dot{T}>$ 2.0 K/s. In contrast, another study showed that the ternary Al-1wt%Fe-1wt%Ni alloy solidified under transient solidification conditions [17], developed only cells along the entire range of examined cooling rates. In contrast,

dendrites prevailed for the binary Al-1.0wt%Ni alloy solidified under similar conditions [20]. This reinforces the need for detailed studies mapping the morphologies and the factors affecting their growth for multicomponent Al-based alloys.

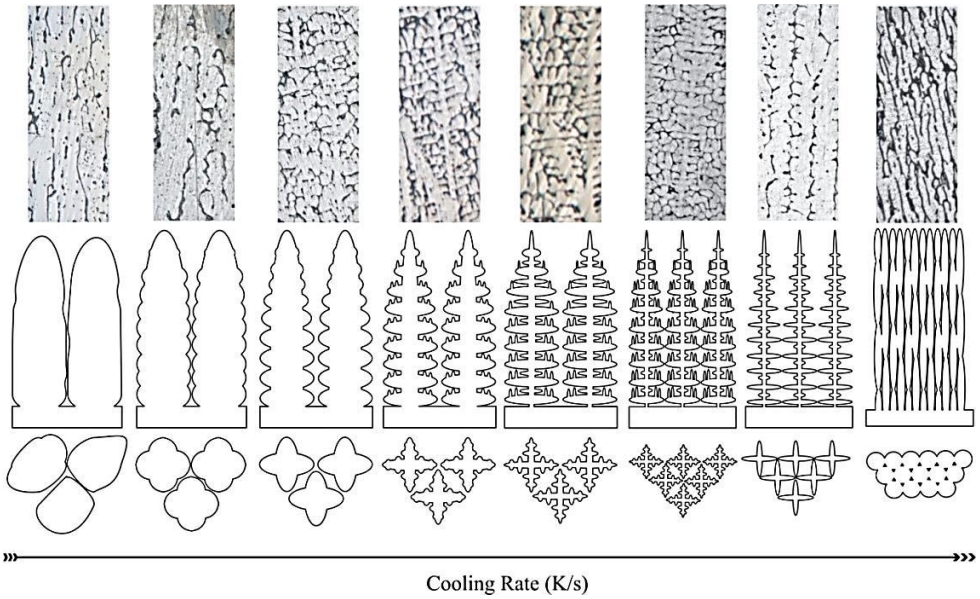

Figure 3 - Schematic progression of α-Al morphologies as a function of cooling rate and representative microstructures of the directionally solidified Al-3wt%Mg-1wt%Si alloy.

In order to compare the experimental growth law $\boldsymbol{\lambda_1 = 126\dot{T}^{-0.55}}$ proposed in the present study, experimental λ_1 data from the literature [21] have been included as open circles in Figure 4. The λ_1 scatter from the literature were related to stationary cooling rates calculated by the expression $\boldsymbol{\dot{T} = G \times v}$, where the growth rate, *v*, ranged from 0.0172mm/s to 0.1 mm/s and the thermal gradient, G, ranged from 0.45 K/mm to 17 K/mm. These λ_1 data are compared with the experimental growth law (Figure 1) for the dendritic region derived in the present work. An excellent agreement can be observed between the present results and the results from the literature, despite differences in the alloys compositions. The good fit observed demonstrated that the -0.55 exponent can also be applied in the case of another Al-Mg-Si alloy composition, being valid for both steady-state and unsteady-state solidification conditions. This gives indications that the experimentally derived scaling laws using the present results could be representative of the dendritic growth for other Al-Mg-Si alloy compositions.

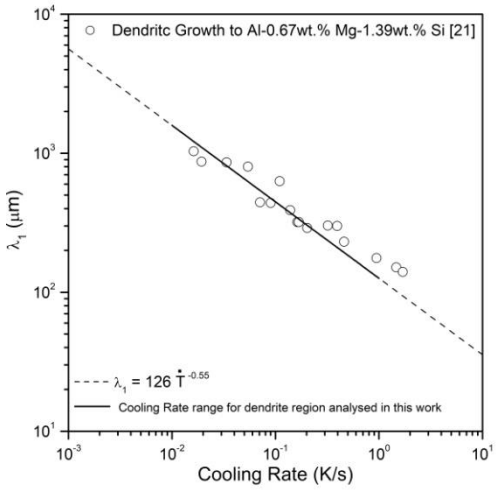

Figure 4 - Comparison of experimental steady-state results [21] showing λ_1 as a function of $\dot{T}$ in the present study and for another ternary Al-Mg-Si alloy.

4. Conclusions

The effect of the cooling rate on the morphology of the α-Al matrix was examined for Al-3wt%Mg-1wt%Si alloy samples solidified upon a wide range of solidification conditions. For this purpose, directional solidification experiments were conducted using a Bridgman (steady state) device and another device that allows the solidification under transient conditions (unsteady state). Consequently, a broad range of solidification cooling rates ($\dot{T}$), varying from 0.003K/s to 45K/s could be assessed as well as the corresponding microstructures. This combination of techniques led to the identification of a complete cycle of α-Al morphologies from cells to dendrites and reverting from dendrites to cells. The range of experimental cooling rates associated with the steady-state experiments was 0.003K/s < $\dot{T}$ <0.17K/s. For cooling rates between 0.03K/s and 0.17K/s only dendritic morphologies prevailed. For $\dot{T}$ values lower than 0.005K/s a degenerate growth of α-Al cells was observed. For unsteady state conditions, the range of experimental cooling rates was 0.2K/s < $\dot{T}$ < 45K/s. The observed growth of high cooling rate cells was related to $\dot{T}$ > 2K/s whereas the dendrites prevailed for $\dot{T}$ < 0.8K/s. Values in between refer to a zone in which both cells and dendrites could be found. Experimental scaling laws were proposed correlating both λ_C and $\lambda_1$with$\dot{T}$. It is worth noting that the same power function law could be found for all laws related to cell, primary and secondary dendrite spacings.

ACKNOWLEDGMENTS

The authors acknowledge the financial support provided by FAPESP (Grants 2012/08494-0; 2012/16328-2, 2013/23396-7 and 2014/25809-0), CNPq and CAPES/COFECUB (Grant 23038.000069/2015-04).

References

[1] Hunt JD and Lu SZ. 1996. *Metall Mater Trans A*. 27(A) 611-623.
[2] Kurz W and Fisher DJ. 1992. *Fundamentals of Solidification*. (Switzerland: Trans. Tech. Public.) p 87.
[3] Trivedi R, Sekhar JA, Seetharaman V. 1989. *Metall Trans A*. 20(A) 769-777.
[4] Mullins WW and Sekerka RF. 1964. *J Appl Phys*. 35(2) 444-451.
[5] Fu JW, Yang YS, Guo J J, & Tong WH. 2008. *Mater Sci Tech*. 24(8) 941-944.
[6] Lee JH, Kim HC, Jo CY, Kim SK, Shin JH, Liu S, & Trivedi R. 2005. *Mat Sci Eng A*. 413 306-311.
[7] Chikama H, Shibata H, Emi T, & Suzuki M. 1996. *Mater Trans*. 37(4) 620-626.
[8] Brito C, Vida T, Freitas E, Cheung N, Spinelli JE, & Garcia A. 2016. *J Alloys Compd*. 673 220-230.
[9] Rodrigues AV, Lima TS, Vida TA, Brito C, Garcia A, & Cheung N. 2018. *Met Mater-Int*. 24 1058–1076.
[10] Bertelli F, Freitas ES, Cheung N, Arenas MA, Conde A, Damborenea J, & Garcia A. 2017. *J Alloys Compd*. 695 3621-3631.
[11] Jung H, Mangelinck-Noël N, Nguyen-Thi H, Billia B. 2009. *J Alloys Compd*. 484(1-2), 739-746.
[12] Gündüz M, and Çadırlı E. 2002. *Mater Sci Eng A*. 327(2), 167-185.
[13] Goulart PR, Spinelli JE, Cheung N, Mangelinck-Nöel N, & Garcia A. 2010. *J Alloys Compd*. 504(1) 205-210.
[14] Canté, MV, Brito, C, Spinelli, JE, Garcia, A. 2013. *Mater Design*. 51, 342-346.
[15] Brito C, Costa TA, Vida TA, Bertelli F, Cheung N, Spinelli JE, & Garcia A. 2015. *Metall Mater Trans A*. 46(8) 3342-3355.
[16] Peres MD, Siqueira CA, & Garcia A. 2004. *J Alloys Compd*. 381(1) 168-181.
[17] Bertelli F, Brito C, Ferreira IL, Reinhart G, Nguyen-Thi H, Mangelinck-Noël N, Cheung N & Garcia A. 2015. *Mater Design*. 72 31-42.
[18] Canté MV, Brito C, Spinelli JE, & Garcia A. 2013. *Mater Design*. 51 342-346.
[19] Kurz W, and Fisher DJ. 1981. Dendrite growth at the limit of stability: tip radius and spacing. *Acta Metall*. 29(1) 11-20.
[20] Canté MV, Spinelli JE, Ferreira IL, Cheung N, & Garcia A. 2008. *Metall Mater Trans A*. 39(7) 1712.
[21] McCartney DG and Hunt JD. 1981. *Acta Metall*. 29(11) 1851-1863.